Journal of Organometallic Chemistry 880 (2019) 241–252

Contents lists available at ScienceDirect

Journal of Organometallic Chemistry

journal homepage: www.elsevier.com/locate/jorganchem

Homolytically weak metal-carbon bonds make robust controlled radical polymerizations systems for “less-activated monomers”

Christophe Fliedel [a], Rinaldo Poli [a, b, *]

[a] LCC-CNRS (Laboratoire de Chimie de Coordination), Université de Toulouse, CNRS, INPT, UPS, 205 route de Narbonne, Toulouse Cedex 4, 31077, France
[b] Institut Universitaire de France, 1 rue Descartes, Paris Cedex 05, 75231, France

ARTICLE INFO

Article history:
Received 5 October 2018
Received in revised form
4 November 2018
Accepted 7 November 2018
Available online 12 November 2018

Keywords:
Organometallic-mediated radical polymerization
Homolytic cleavage
Metal-carbon bond strength
Catalytic chain transfer
DFT calculations

ABSTRACT

This article is an account of work, mostly carried out in the authors' laboratory, on the use of organometallic compounds with homolytically fragile metal-carbon bonds as dormant species in the controlled radical polymerization of a variety of monomers in what is now universally called “organometallic-mediated radical polymerization” (OMRP). The article retraces a brief history of OMRP, shows how it can potentially intervene in every radical polymerization process based on atom transfer (ATRP), which is a more popular controlling method where the metal plays a catalytic role, and how it can be in competition with another catalyzed process involving chain transfer to monomer (CCT). It highlights the challenges of controlled radical polymerization in the area of the “less activated monomers” (LAMs) and particularly the problem of the monomer addition errors, demonstrating how ligand engineering and coordination chemistry constitute additional handles, not available to other moderating species, providing acceptable *ad hoc* solutions. It details how OMRP could achieve unsurpassed levels of control for two specific monomers: vinyl acetate (VAc) and vinylidene fluoride (VDF). Finally, it lays the principles for the development of efficient chain transfer catalysts for less activated monomers.

Contents

1. Introduction

Alkyl derivatives of the transition metals are the quintessence of organometallic chemistry. Initially developed as curiosities, they are now of great importance since they are recognized to play

* Corresponding author. LCC-CNRS (Laboratoire de Chimie de Coordination), Université de Toulouse, CNRS, INPT, UPS, 205 route de Narbonne, Toulouse Cedex 4, 31077, France.
E-mail address: rinaldo.poli@lcc-toulouse.fr (R. Poli).

https://doi.org/10.1016/j.jorganchem.2018.11.012
0022-328X/

crucial roles in living systems (notably vitamin B12 [1]) and in all catalyzed transformations of organic substrates that result in the functionalization of sp^3-hybridized carbon atoms [2]. Compounds containing a transition metal-alkyl bond are generally prone to facile decomposition by a number of different pathways including protonolysis, aerial oxidation, α- and β-H eliminations, reductive elimination and homolytic cleavage. For these reasons, special care is needed to design alkyl complexes that are sufficiently stable under laboratory conditions to be isolated and characterized [3,4]. In particular, the bond dissociation free energy (BDFE) must be sufficiently high in order to avoid homolytic cleavage with the production of radicals, because the latter spontaneously and quickly (at close to diffusion-limited rates) combine with each other and/or disproportionate. Nevertheless, it has become clear in the last 20 years that organometallic compound with homolytically weak metal-carbon bonds may play a crucial role in controlled radical polymerization, providing unique features that make them preferred controlling agent for certain monomers.

Controlled radical polymerization, also known as Reversible Deactivation Radical Polymerization (RDRP) [5], has now become a preferred tool for the fabrication of functional polymers by macromolecular engineering [6]. It gives access to size- and distribution-controlled and chain-end-functionalized macromolecules under mild conditions for a wide variety of monomers and is compatible with most any reaction medium, including water. It rests on either one of two distinct strategies: reversible termination (RT, see Scheme 1) and degenerative transfer (DT, see Scheme 2). Each one of these allows chain growth while greatly reducing the impact of spontaneous bimolecular radical terminations.

In RT methods, the active radicals are generated from a dormant species by reversible bond cleavage with an activation rate constant k_a, producing at the same time a radical trapping species T, also called "moderating agent" or "persistent radical" (although it does not necessarily need to either have radical character or to be persistent [7]). The latter remains available to trap the growing chains and regenerate the dormant species with a deactivation rate constant k_{da}. The active radicals also add to monomer to extend the chain with the propagation rate constant k_p and undergo irreversible bimolecular terminations with the termination rate constant k_t. The pseudo-equilibrium between active and dormant chains ($K = k_a/k_{da}$) is suitably placed to significantly reduce the free

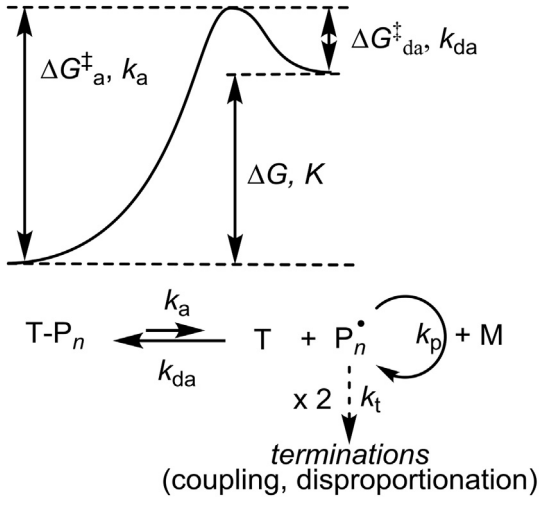

Scheme 1. Mechanism and activation/deactivation free energy profile of a controlled radical polymerization based on reversible termination. P_n = polymer chain with degree of polymerization n, T = radical trapping species, M = monomer.

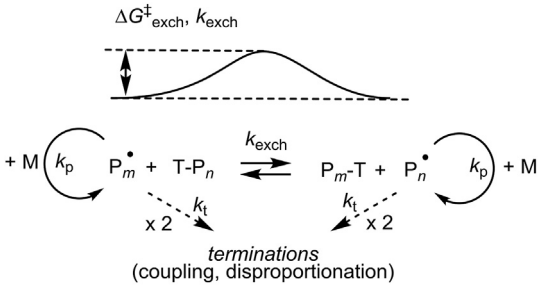

Scheme 2. Mechanism and free energy profile of a controlled radical polymerization based on degenerative transfer. The symbols have the same meaning as in Scheme 1.

radical concentration, rendering the chain extension process slow ($v_p = k_p[P^\bullet][M]$, where $[P^\bullet] = \sum_n [P_n^\bullet]$) and the terminations even slower ($v_t = k_t[P^\bullet]^2$), thus reducing the impact of termination over propagation: $v_t/v_p = (k_t/k_p)([P^\bullet]/[M]) = (k_t/k_p)(K[P_n\text{-}T]/[T][M])$. This is widely known as the "persistent radical effect" [8]. A variety of species T have been successfully used; our interest here is limited to transition metal complexes ($T = Mt^x/L$ where Mt = metal, x = formal oxidation state and /L = coordination sphere). Therefore, the dormant species is organometallic, with a metal-carbon bond at the chain end, $P_n\text{-}Mt^{x+1}/L$. Whereas the steady-state $[P^\bullet]$ in free radical polymerization is usually in the $10^{-7} - 10^{-8}$ M range, a typical controlled process features lower concentrations by 2–4 orders of magnitude, which is insured by equilibrium constants K of the order of $10^{-9} - 10^{-14}$, depending on temperature. This requires a BDFE in the 12–20 kcal/mol range, namely a rather weak bond. Equilibrium constants that are even lower than the above range, associated to stronger bonds for the dormant species, yield too low free radical concentrations. In that case, even though leading to better control (lower impact of irreversible terminations), the polymerization process becomes impractically slow and a compromise has to be found.

In degenerative transfer methods, the active radical is liberated from the T-P_n dormant species by exchange with another like radical, hence in an associative manner. This dormant species acts in this case also as a reversible and degenerate chain transfer agent, like in immortal polymerization processes [9]. There is no persistent radical effect and no moderating species is present to reduce the active radical concentration. Rather, a standard radical initiator must be present to continuously inject a small flux of new radicals into solution. Hence, the reaction follows the free polymerization kinetics and the impact of the bimolecular terminations is not reduced. However, the chains grow in a controlled fashion provided that the associative exchange ($v_{exch} = k_{exch}[P^\bullet][T\text{-}P]$) is much faster than the propagation ($v_p = k_p[P^\bullet][M]$), namely $k_{exch}[T\text{-}P] \gg k_p[M]$. The process can essentially be considered as a quasi-immortal polymerization. As in the RT methods, the role of the fragment T in DT methods can be played by a transition metal complex, namely the dormant species/chain transfer agent can be an organometallic species $P_n\text{-}Mt^{x+1}/L$. Since the bond being broken is compensated by the formation of an identical bond, the metal-carbon bond strength (*i.e.* the BDFE) is not necessarily an issue here. The only important criterion is to have a very fast degenerative exchange process. However, when applied to the controlled polymerization of less activated monomers (more on this in section 4), bond strength considerations do become important when the monomer is asymmetric, as will be shown in that section. Another key structural parameter that makes a metal complex successful is the presence of a vacant coordination site, ideally placed *trans* to the existing P_n ligand in order to avoid the competing reductive elimination process.

The use of transition metal complexes as moderating species in RDRP, generating an organometallic dormant species, whether operating by the RT or by the DT approach, has been termed "organometallic-mediated radical polymerization" (OMRP) [10] and a number of reviews have previously been published [11–20]. This article will retrace a few of the leading concepts and underline the specificity of the technique on the basis of a few of the most recent results.

2. Brief history of OMRP

The first use of a metal complex as a reversible trap for polymer radical chains, operating by the RT strategy, appeared in 1994, nearly simultaneously and under different conditions from two research groups. Acrylates were radically polymerized with controlled growth either in the presence of neopentyl(tetramesitylporphyrin)cobalt(III) with thermal activation at 60 °C [21] or in the presence of alkylcobaloximes with photolytic Co–C bond cleavage at room temperature [22,23]. The principle of control for a radical photopolymerization process had in fact already been announced in 1992 for a study with a (porphyrin) rhodium(II) system [24]. While excellent control was achieved by the thermal process with the porphyrin system (degree of polymerization up to 2000 with M_n close to target and relatively low disperities of 1.1–1.3) [21,25], the cobaloxime photopolymerization led to polymers with molecular weights lower than target and broader molecular weight distributions, caused by competing chain transfer processes, particularly for lower monomer/cobalt ratios [22,23]. An analysis of the mechanistic issues and the achievement of control in photo-OMRP processes has been reported much more recently [26]. These discoveries were made in the realm of intense studies of catalytic chain transfer (CCT), an area of keen industrial interest, whereby the addition of small amounts of a metal complex to a free radical polymerization system may catalyze chain transfer to monomer, with the generation of short polymer chains characterized by unsaturated chain ends [27,28]. The process occurs by transfer of a β-H atom from the radical chain to the reduced Mt^x/L catalyst, producing an unsaturated dead chain and the hydride complex H-Mt^{x+1}/L. The latter then initiates the growth of a new chain by transferring the H atom to a monomer molecule, see Scheme 3. Note that the formation of direct metal-carbon bonds does not occur in CCT, hence this phenomenon is, *stricto sensu*, not organometallic. Complexes based on cobalt are the most active catalysts for this process. Note that the slow step of CCT (β-H atom transfer) and the OMRP trapping (direct P_n-Mt^x/L bond formation) involve the same two partners, Mt^x/L and $P^{\bullet}_n$, and are therefore in direct competition with each other. Since these early reports, many other cobalt(II)/alkylcobalt(III) systems able to promote polymer chain growth in a controlled fashion with low or no impact of CCT have been reported and, to this day, continue to dominate the OMRP research activity [11]. However, several other metals, particularly iron [16] but also molybdenum, titanium, vanadium and others, have been investigated as well [11–19].

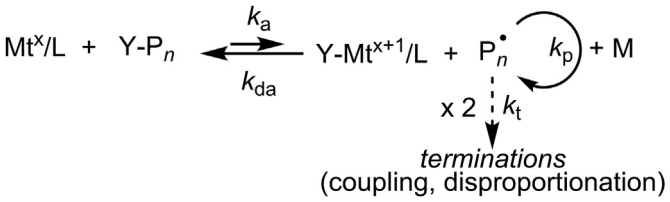

Scheme 4. Mechanism of atom transfer radical polymerization. Y = halogen atom. The other symbols have the same meaning as in Scheme 1 and Scheme 3.

The pioneering publications highlighted above actually appeared before the first reports of the much more popular "atom transfer radical polymerization" (ATRP) [29,30], a catalytic process that functions by the reversible termination protocol (see Scheme 4) where halogen-capped dormant species are activated by a reduced transition metal complex Mt^x/L. ATRP has immediately gained much more popularity than OMRP [31], partly because it is more practical and flexible in terms of initiator choice and stability, but especially because the transition metal complex acts catalytically without being chemically linked to the polymer chain. In OMRP, on the other hand, the recovered polymer has the metal covalently bonded as chain-end functionality. Therefore, in addition to the increased cost of the moderating agent, costly and time consuming post-modifications are necessary if metal-free polymers are desired. Indeed, there has been essentially no further contribution to the OMRP area until we discovered in 2001, using molybdenum systems, that the OMRP trapping equilibrium interplays not only with CCT but also with the ATRP equilibrium [32]. A qualitative energy profile illustrating the interplay of the three processes is shown in Fig. 1. Other systems displaying various types

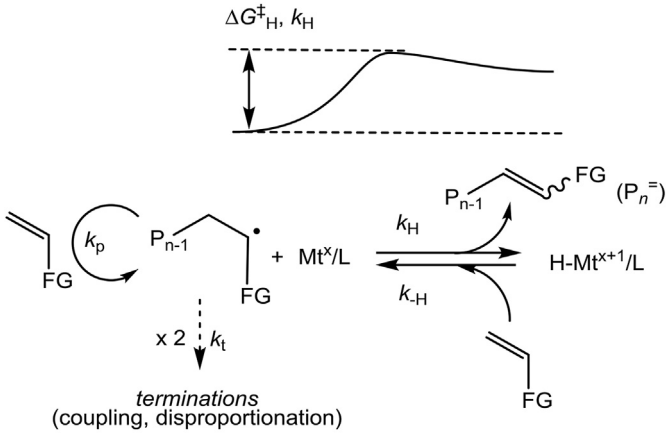

Scheme 3. Mechanism and free energy profile of metal-catalyzed chain transfer to monomer (CCT). FG stands for "functional group". Mt = metal, x = formal oxidation state, /L = coordination sphere. P_n has the same meaning as in Scheme 1; P_0 = H.

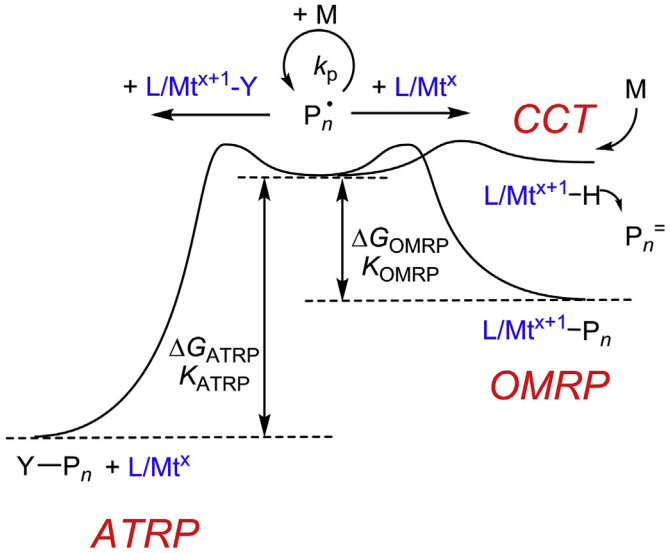

Fig. 1. Interplay between ATRP, OMRP and CCT processes. All symbols are defined in the schemes and within the text.

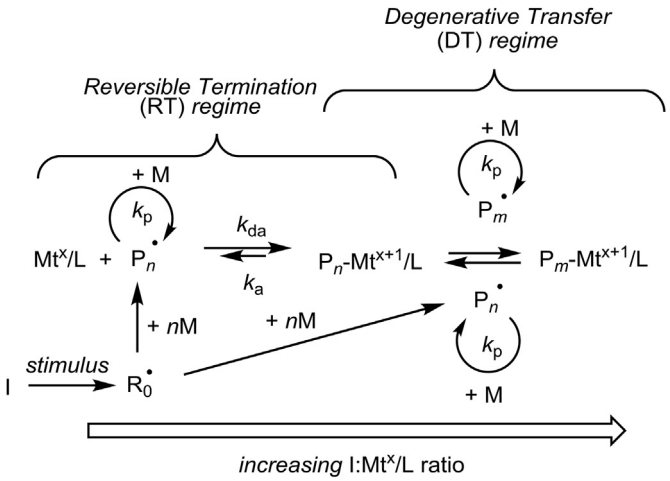

Scheme 5. Interplay of RT and DT OMRP when starting the polymerization with a dual initiating system. I = initiator, R_0 = primary radical. The other symbols have the same meaning as in Scheme 1 and Scheme 3.

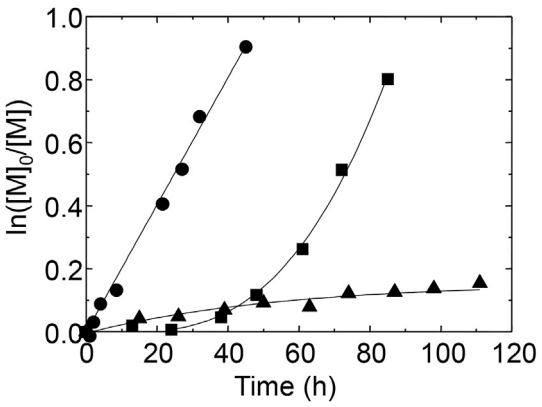

Fig. 2. Effect of the addition of external ligands (L) to kinetics of the bulk OMRP of VAc mediated by [Co(acac)$_2$] with V-70 at 30 °C ([VAc]$_0$/[Co(acac)$_2$]$_0$/[V-70]$_0$/[L]$_0$ = 500:1:1:30). (■) no addition, (●) addition of py (30 equiv), (▲) addition of NEt_3 (30 equiv). Reproduced with permission from Ref. [45]. Copyright 2007 Wiley-VCH.

of mechanistic interplays have been reported later, for instance an osmium system featuring ATRP/OMRP [33,34], an iron system with ATRP/CCT [35–37], and yet another iron system with ATRP/OMRP [38–40].

The first degenerative transfer OMRP was disclosed only in 2004, once again based on an alkyl(porphyrin)cobalt(III) system, for the controlled polymerization of acrylate monomers [41]. The same contribution has also highlighted the interplay between OMRP-RT and OMRP-DT approaches. There are two ways, in principle equivalent, to initiate an OMRP, using either a unimolecular R_0-Mt^{x+1}/L initiator or a dual initiating system consisting of Mt^x/L and a conventional radical initiator that generates the primary radical $R_0^\bullet$ *in situ*. When using the second approach, the system operates under the OMRP-RT regime so long as the amount of produced primary radicals is substoichiometric relative to Mt^x/L, but switches to the DT regime when the radicals exceed the metal amount, see Scheme 5. The alternative initiation method using an unimolecular organometallic initiator, on the other hand, can only operate under the RT regime as the radicals can never exceed the metal amount, although the addition of a conventional radical initiator to an organometallic R_0-Mt^{x+1}/L species led to an OMRP-DT process without induction period [42]. The interplay of RT and DT in OMRP has only been shown, to the best of our knowledge, with cobalt complexes as moderating species. The same interplay has also been shown for main group elements in organotellurium-mediated radical polymerization (usually referred to as TERP) [43].

3. The importance of ligand coordination in OMRP

Coordination chemistry (ligand engineering) is of great aid in the modulation of OMRP for three reasons. Firstly, the steric encumbrance of the ligand coordination sphere modulates the Mt–C bond strength in RT methods. Secondly, vacant coordination sites that become available by chain release from the dormant species can be occupied by external ligand, modulating the dissociation equilibrium. Thirdly, the vacant coordination site needed for the associative radical exchange in the DT regime may also be occupied by external ligands, negatively affecting or even completely blocking the associative radical exchange. The effect of sterically induced bond labilization is one of the main interests in the OMRP technique for the control of less activated monomers and will be analysed more in details in the next section. We will discuss here the other two effects on the basis of the OMRP of vinyl acetate (VAc) moderated by [Co(acac)$_2$] (acac = acetylacetonate).

This controlled polymerization was first reported with dual initiation by V-70 and [Co^{II}(acac)$_2$] in bulk at 30 °C. V-70 is the trade name of 2,2′-azobis(4-methoxy-2,4-dimethylvaleronitrile), a diazo compound with a half-life of 10 h at this temperature. There is a long induction period before a rapid phase of controlled polymerization [44], during which the initially formed short $R_0(VAc)_n^\bullet$ chains ($n \sim 4$) are trapped irreversibly to form [$R_0(VAc)_nCo^{III}$(acac)$_2$] species that are not reactivated under these conditions, because the Co-PVac bond is too strong (more on this below). Indeed, the generated metal-capped oligomeric chains have been isolated and characterized [42], and later used as efficient unimolecular initiator. With the dual initiating system, after the induction period and the quantitative conversion of [Co^{II}(acac)$_2$] to [$R_0(VAc)_nCo^{III}$(acac)$_2$], the polymerization is triggered by the excess radicals via degenerate transfer (Scheme 5). Addition of external monodentate ligands (pyridine, water, DMF, DMSO, etc.) to the medium, however, switches the polymerization from the DT to the RT regime while maintaining a controlled chain growth [45,46]. This is shown quite clearly by the elimination of the initial induction period, see Fig. 2. The activation of the RT pathway is made possible by the greater stabilization of the "persistent radical" species, [Co(acac)$_2$], through formation of [Co(acac)$_2$(L)$_2$], relative to the stabilization of the dormant species through formation of [Co(acac)$_2$(P_n)(L)]. The faster polymerization in the presence of pyridine relative to NEt_3 results for the stronger coordinating power of the former ligand, increasing the K_{OMRP} for the moderating RT equilibrium [45]. Another study has shown that K_{OMRP} increases in the order L = DMF < DMSO < H_2O [46]. Fig. 2 also shows that when [Co(acac)$_2$] is completely converted into [Co(acac)$_2$(PVAc)], namely at the onset of the DT polymerization in the absence of added ligands (end of the induction period), the slower RT polymerization in the presence of NEt_3 continues at the same rate instead of speeding up like the DT polymerization. This demonstrates the blocking effect of ligand coordination, making it impossible to sustain the degenerate transfer mechanism. All new radicals produced by the excess initiator rapidly terminate, while the monomer continues to be slowly incorporated into the longer Co(acac)$_2$-capped chains in a controlled manner.

This ligand coordination effect is often neglected or overlooked. For instance, the polymerization of VAc was recently studied under similar conditions to those mentioned above, in bulk at 60 °C with dual initiation, using three different Co^{II} complexes and AIBN as a

source of primary radicals ($t_{1/2}$—6 h at this temperature) [47]. With the [Co^{II}(TMP)] and [Co^{II}(salen*)] moderators (TMP = tetramesitylporphyrin; salen* = *N*,*N*′-bis(3,5-di-*tert*-butylsalicylidene)-1,2-cyclohexanediamine) the observed behavior is identical to that originally reported for the [$Co^{II}(acac)_2$]/V-70 dual initiator at 30 °C, with an induction period lasting until all the [L/Co^{II}] moderating complex is transformed into the [L/Co^{III}—PVAc] dormant species (ca. 45000 s or 12.5 h, see Fig. 3). This behavior is rationalized by the irreversible radical trapping in the RT regime, followed by a fast and controlled polymerization in the DT regime (Scheme 5). The [$Co^{II}(acac)_2$]-mediated polymerization, on the other hand, gave rise to a shorter induction time (ca. 20000 s or 5.6 h) and an initially faster polymerization, see Fig. 3. The authors of this contribution attributed this difference to the intervention of the RT mechanism, proposing that "the raised polymerization temperature weakened the Co—C bond in the organocobalt(III) species and shifted the mechanism from DT to RT" [47]. However, if this were true, this scenario should be valid from the very beginning of the polymerization. We rather consider it more likely that this phenomenon results from contamination of the [$Co^{II}(acac)_2$] mediating agent, which is more hygroscopic than the TMP and salen* complexes, by [$Co^{II}(acac)_2(H_2O)_2$]. During the induction period, the anhydrous [$Co^{II}(acac)_2$] irreversibly traps the radicals. Then the polymerization starts by the DT mechanism, through the anhydrous [Co^{III}(PVAc)] dormant species, and the polymerization is faster simply because the radical flux from AIBN after 20000 s is greater than after 45000 s. In this regime, the [$Co^{II}(acac)_2(H_2O)_2$] contaminant can also assist by reversibly trapping the radical chains and therefore the target degree of polymerization should correspond to the molar ratio between the monomer and the overall cobalt amount.

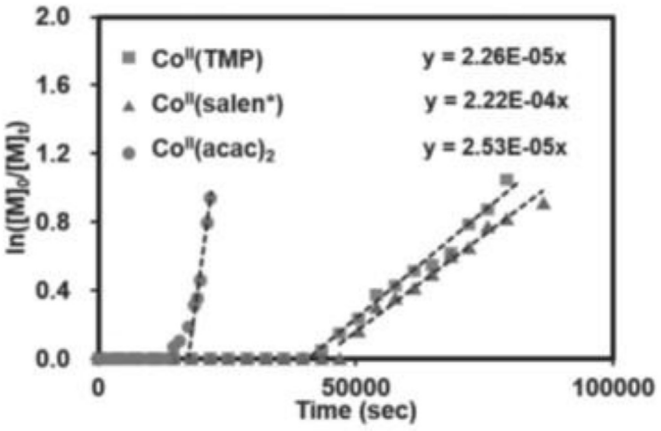

Fig. 3. First order kinetic plot for the bulk VAc polymerization mediated by different cobalt(II) complexes with AIBN at 60 °C ($[VAc]_0/[Co^{II}]_0/[AIBN]_0 = 700:1:3$). Reproduced with permission from Ref. [47]. Copyright 2016 Wiley-VCH.

4. The challenge of less activated monomers. Part 1: the BDE issue in RT methods

Monomers that belong to the family of so-called "more activated monomers" (MAMs) have been successfully controlled by several methods, whether they operate by RT or DT. These include styrenics, acrylates, methacrylates, acrylamides, and other monomers that are associated with stabilized radicals, namely radicals that benefit from π delocalization of the unpaired electron. While the moderating agents "protect" the reactive radicals in the dormant state, propagation may only occur while the chain is in the free radical state, thus same reactivity as in free radical polymerization is observed, see Fig. 4. The reactivity of the monomer in radical polymerization is inversely proportional to that of the associated radical. The monomers on the right hand side of this scale, associated to the more reactive radicals, are usually referred as "less activated monomers" (LAMs) and represent a challenge for controlled radical polymerization. It is important to underline that the term "less activated", widely used by the polymer community in reference to this radical reactivity scale, is specific for radical polymerization. Different polymerization mechanisms lead to different reactivity scales.

Is it easy to understand why LAMs are a challenge for the RT methods. The dormant species must be activated dissociatively by homolytically cleaving the P_n-T bond. The free radicals associated to LAMs are more reactive and produce homolytically stronger bonds with the moderating agent, slowing down the activation process. For a successful RT polymerization of these monomers, moderating agents T that naturally form very weak bonds are needed. This is where metal complexes become of interest. As already stated, the catalytic ATRP is more interesting than the stoichiometric OMRP. The cost of homolytically breaking the bond between the latent radical and the capping species T (a halogen atom in ATRP) is compensated by the formation of a new bond between the halogen atom and the metal atom (Scheme 4). The free energy change for the ATRP activation equilibrium is $\Delta G_{ATRP} = BDFE(C{-}Y) - BDFE(Mt^{x+1}\text{-}Y)$. Although equilibria are related to the reaction free energy change, homolytic bond strengths are more frequently assessed through the bond dissociation enthalpies (BDE), since these are often experimentally accessible through calorimetry,

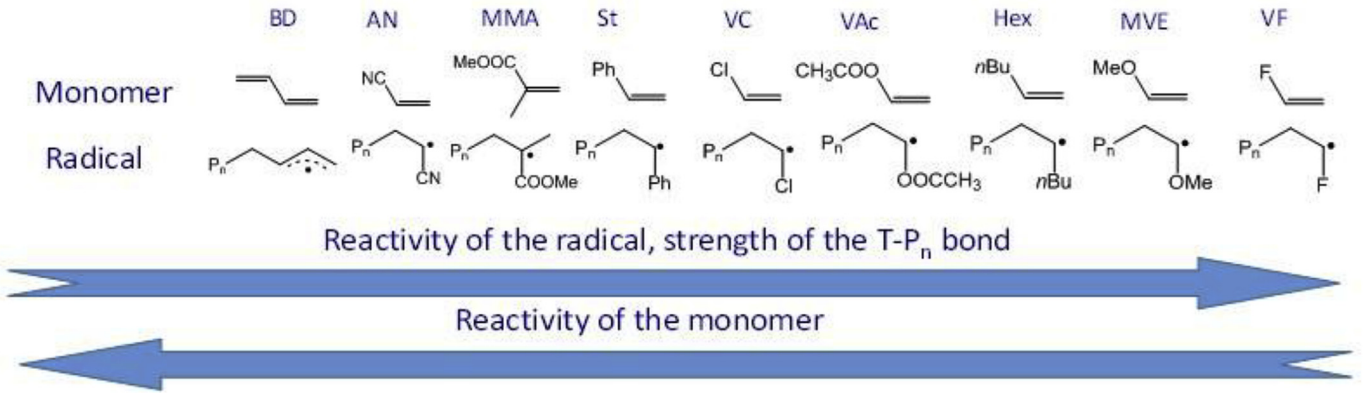

Fig. 4. Qualitative reactivity order of a few representative radical chains and of their associated monomers. BD = 1,3-butadiene; AN = acrylonitrile; MMA = methyl methacrylate; St = styrene; VC = vinyl chloride; VAc = vinyl acetate; Hex = 1-hexene; MVE = methyl vinyl ether; VF = vinyl fluoride.

photoionization mass spectrometry, and other methods [48]. Using an activating metal complex able to make a stronger Mt^{x+1}-Y bond should compensate the cost of cleaving a stronger C–Y bond. However, having at the same time a more reactive radical and a more reactive metal with *a fortiori* render more favorable the formation of the organometallic dormant species P_n-Mt^{x+1}/L and switch the controlling mechanism, via the interplay shown in Fig. 1, from ATRP to OMRP [10,14,18]. For this reason (in addition to other criteria discussed further below) OMRP is more promising than ATRP for the application to LAMs. Note also that, whereas using ATRP conditions always leads to the contribution of OMRP trapping, using OMRP conditions does not lead to interplay with the ATRP mechanism if no halogens are present in the system. However, OMRP may always potentially interplay with CCT (Fig. 1).

OMRP is more interesting than other RT methods for the application to a LAM polymerization because the P_n-Mt^{x+1}/L bond in the dormant species may be sterically labilized by ligand engineering. Nitroxide-mediated polymerization (NMP, a popular RT controlling methods where T = $R_2NO^{\bullet}$) is less flexible in this respect, even though steric effects from the nitroxide R groups do have an impact on the O–C bond strength in the dormant species [49]. We have demonstrated the impact of ligand steric effects on the OMRP of VAc, a typical LAM, in two different occasions. Using the half-sandwich [$CpCr^{II}(nacnac^{Ar,Ar})$] complex as a moderating species, where $nacnac^{Ar,Ar}$ is the β-diketiminate ArNC(Me)CHC(Me)NAr, in combination with a diazo compound in a dual initiating system operating under the RT regime (primary radical/Cr < 1), the polymerization is much faster for the bulkier Ar = 2,6-diisopropylphenyl (Dipp) system than for the analogous one with Ar = 2,6-dimethylphenyl (xylyl) [50,51]. DFT calculations suggest that the Cr^{III}–PVAc BDE for the Dipp system is 2 kcal/mol lower than for the xylyl system and >7 kcal/mol lower than for the simpler system with unsubstituted phenyl groups.

The second example is the bis(β-diketonate)cobalt system, again for the VAc polymerization. Using [$Co^{II}(acac)_2$] and V-70 as dual initiating system for a bulk polymerization at 30 °C, there is a long induction time before a rapid phase of controlled polymerization by degenerative transfer (Scheme 5) as already detailed in the previous section [44]. The Co^{III}–PVAc bond in the [$R_0(VAc)_n$-$Co^{III}(acac)_2$] dormant species is too strong (more on this below) and is not reactivated under these conditions. Moving to the bulkier 2,2,6,6-tetramethylheptanedionate (tmhd) ligand, [*t*BuC(O)CHC(O)*t*Bu]$^-$, namely using [$Co^{II}(tmhd)_2$] instead of [$Co^{II}(acac)_2$], the results are similar under bulk monomer conditions. However, running the polymerizations in toluene (50% v/v), which slows down propagation, leads to only partial monomer conversion at the end of the V-70 initiator lifetime (ca. 7 half-lives, *i.e.*70 h at 30 °C). Under these conditions, the behavior of the two complexes is different: whereas the kinetics is approximately identical during the induction time and during the subsequent DT regime, after ca. 70 h the polymerization returns to the RT regime and slows down dramatically in the presence of [$Co^{II}(acac)_2$], while it continues at a faster rate in the presence of [$Co^{II}(tmhd)_2$], see Fig. 5. The DFT calculations suggest that the Co^{III}–C BDE in [$(tmhd)_2Co^{III}$–PVAc] is 1.4 kcal/mol weaker than in [$(acac)_2Co^{III}$–PVAc] (15.8 *vs.* 17.2 kcal/mol) [52].

The [$Co(acac)_2$] controlling agent is rather special for the OMRP of LAMs, mostly thanks to the labilizing effect of ligand coordination detailed above in section 3, but also because of intrinsically weaker Co^{III}–C bonds than for related systems with a nitrogen-based coordination sphere (porphyrins, Schiff bases, etc.). While the latter are suited to the OMRP-RT of MAMs and lead to irreversible trapping of LAMs (although VAc has been controlled in the DT regime by porphyrin [53,54] and Schiff base [47] complexes), [$Co(acac)_2$] is able to control the polymerization of VAc and also, as will be shown later in section 8, vinylidene fluoride (VDF) in the RT regime in the presence of donor ligands. On the other hand, it is not able to trap MAMs as efficiently because the Co^{III}–C bond is too weak, leading to lower degrees of control, as shown for instance for the polymerization of *n*-butyl acrylate [55].

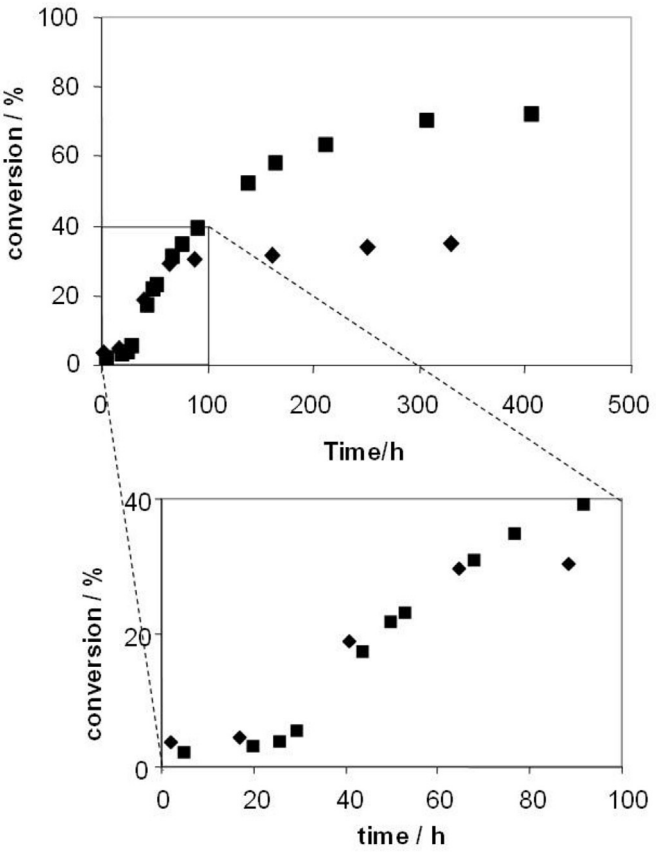

Fig. 5. Time dependence of $\ln([M]_0/[M])$ for polymerization of VAc at 30 °C in toluene solution (50% v/v). VAc/V-70/Co = 500/2/1. Squares: polymerization mediated by [$Co^{II}(tmhd)_2$]; diamonds: polymerization mediated by [$Co^{II}(acac)_2$]. Reproduced with permission from Ref. [52]. Copyright 2009 Wiley-VCH.

5. The challenge of less activated monomers. Part 2: the inverted monomer addition issue in RT methods

In addition to the bond strength problem, the ability of metal complexes to control the polymerization of LAMs by an RT strategy is also affected by a more subtle problem, whenever the monomer molecule features chemically different alkylidenes across the unsaturation. These two moieties are called “head” and “tail”, the former usually referring to the more substituted alkylidene. For instance, in an acrylate ester the CH(COOR) group is the head and CH_2 is the tail. This problem affects also the control by any other moderating species T, but metal complexes offer corrective measures that are not available to the other species.

As is well known from polymer chemistry introductory courses, stabilized radicals are formed more rapidly than less stabilized ones. Therefore, MAMs yield a strictly regular chain with 100% head-tail additions because the head end of the monomer yields a much more stabilized radical than the tail end. This is, however, not the case for LAMs, because of a much lower stability differential. Consequently, the propagation induces a significant fraction of monomer addition errors. The head-tail (regular) addition usually dominates and generates head radicals, but there are significant head-head (inverted) additions, leading to isomeric tail radicals, see

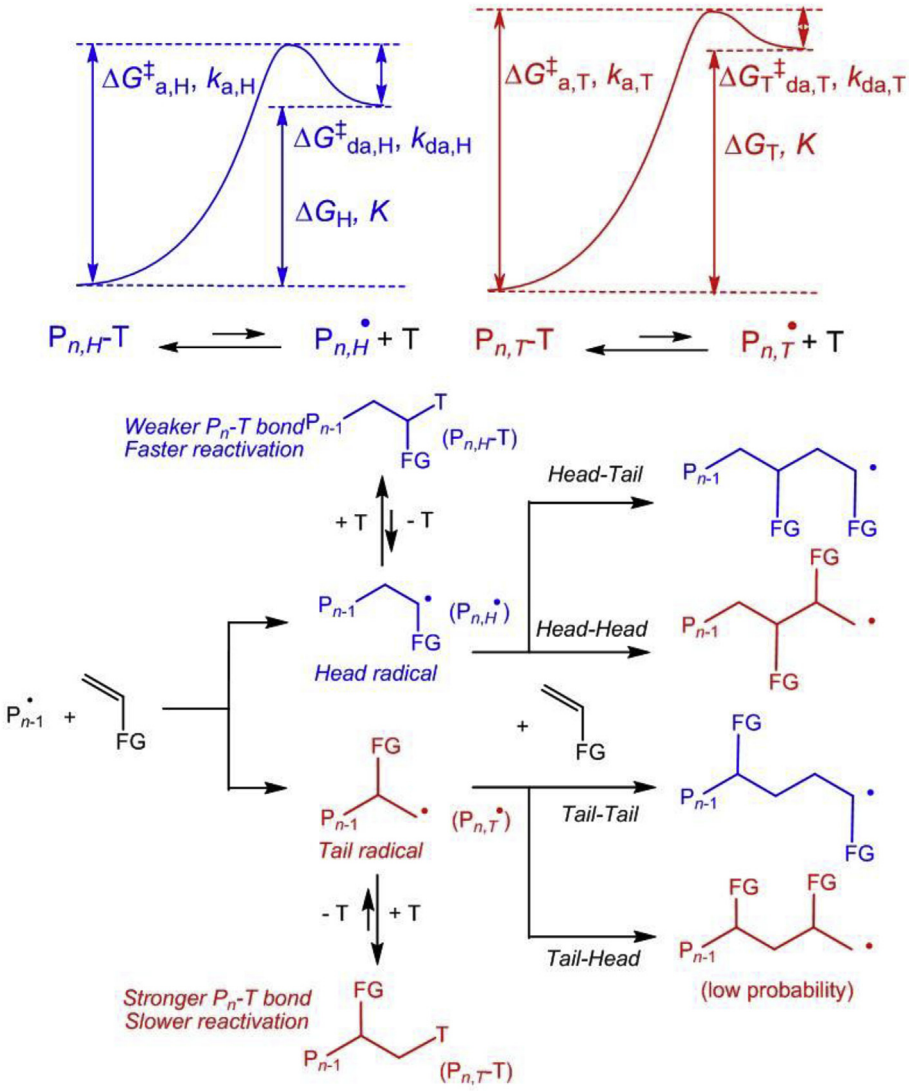

Fig. 6. The problem of the inverted monomer additions for LAMs.

Fig. 6. For instance, depending on conditions (mostly temperature), there may be 1–2% of inverted monomers in a poly(vinyl acetate) chain [56] and 4–5% in a poly(vinylidene fluoride) (PVDF, the VDF monomer is $CH_2{=}CF_2$) [57]. These fractions are obviously the same whether the polymerization is conducted as a free radical or as a controlled radical process, since the key propagation step always occurs on the free radical. The inverted monomer addition problem not only introduces random irregularities in the macromolecule, impacting the materials properties. In controlled polymerizations based on the RT strategy, the more reactive tail radical generates a stronger bond in the dormant species (Fig. 6), which is therefore less easily reactivated and accumulates in the medium. This leads to a slowdown, possibly even a complete stop, of the polymerization. This phenomenon was observed, for instance, for the above-cited OMRP of VAc controlled by the half-sandwich [$CpCr^{II}$(-nacnac^{Xyl,Xyl})] system [51] and also for other attempts to polymerize VAc by other RT strategies [58–60]. The key to avoid this slowdown phenomenon is to equilibrate the P_n-T bond strengths in the two isomeric dormant species, which is not a trivial thing to do for most RDRP-RT methods. In OMRP-RT, two different *ad hoc* solutions have so far been found. The first one is based on chain chelation for the polymerization of VAc and will be detailed in section 7. The second one, which provides the needed corrective measure for the polymerization of VDF, is based on polarity effects on the Mt^{x+1}-P_n bond strength, see section 8.

6. The challenge of less activated monomers. Part 3: DT methods

Since the degenerative transfer methods do not involve dissociative cleavage of the P_n-T bond but rather simultaneous cleavage and formation of equivalent bonds, the P_n-T bond strength should not be a critical issue so long as the associative exchange rate (k_{exch}, Scheme 2) is high and thus DT methods are in principle suited to control the polymerization of LAMs. This is indeed true, but only when the monomer is symmetric. For instance, a controlled polymerization of ethylene, $CH_2{=}CH_2$, has been achieved by the RAFT technique [61] (RAFT = reversible addition-fragmentation chain-transfer), a DT method that makes use of a thiocarbonylthio system as transfer agent [P_n-S–C(S)Z; *e.g.* dithiocarboxylate if Z = alkyl or aryl, dithiocarbamate if Z = dialkylamino, *etc.*]. Significant amounts of ethylene, up to >50% molar, could also be incorporated in a controlled fashion in EVA (ethylene/vinyl acetate random copolymer) by OMRP with the [$Co(acac)_2$] system, although this

polymerization took place under the RT regime [62]. When the monomer is asymmetric, however, the inverted monomer additions lead again to trouble. The reason is that while exchange of the majority head dormant chain, $P_{n,H}$-T, with the majority head radical, $P^{\bullet}_{m,H}$, is degenerative, the isomeric tail radical generated by an inverted monomer addition, $P^{\bullet}_{n,T}$, leads to a non-degenerative exchange with formation of a more stable dormant species, $P_{n,T}$-T, which cannot be easily reactivated by the next majority head radical, see Fig. 7. This more stable tail dormant species therefore tends to accumulate in the system. It may be reactivated by the more reactive tail radical (the tail-tail exchange is again degenerative), but the latter is present only as a minor fraction. Therefore, even though the $k_{exch(TT)}$ rate constant may be high, the rate of exchange ($v_{exch} = k_{exch(TT)}[P_T\text{-T}][P^{\bullet}_T]$) will be low because the radical concentration is low. Contrary to the RT methods where inverted monomer additions lead to a slowdown of the polymerization, these inverted additions slow down only the associative exchange rate, not the polymerization. Slowdown of the exchange rate leads to a loss of control.

This situation is commonly observed when DT methods are applied to the controlled polymerization of asymmetric LAMs. For instance, while the RAFT technique using xanthates (P_n-S–C(S)Z species with Z = OR) as transfer agents leads to reasonable control for the polymerization of VAc [63] and VDF [64], this control is accompanied by a steady increase of polymer dispersity with conversion, which is opposite to the expected behavior and is a signal of decreasing control. The ITP method (iodine transfer polymerization, using P_n-I as chain transfer agents) yields similar results [65,66]. A more detailed study of the polymer evolution for the RAFT of VDF has shown that the $PVDF_T$-SC(S)OEt dormant chains, initially a minority, steadily accumulate until they represent 100% of the sample, at which point the polymerization becomes uncontrolled and thus the technique efficiency is limited to low conversions and short chains [67].

Fig. 8 shows how the thermodynamics of the non-degenerative head-tail radical exchange is equivalent to the BDFE difference of head and tail dormant species. Therefore, the key to achieve an equally facile reactivation of both the major head and the minor tail dormant species is the same as for the RT methods, namely the strengths of the P_n-T bonds in the two isomers must be equilibrated.

7. Effect of chain chelation in the OMRP of VAc

On the basis of the contents of sections 4-6, it is easy to rationalize the failure of most RDRP techniques to achieve a well-controlled polymerization of VAc. Indeed, most reported attempts to obtain chain-end-functionalized PVAc-T polymers with targeted molecular weights and low dispersity, whether using an RT or a DT methods, yielded polymers with decent control only at low conversions, with slowdown behavior for the RT methods, low number-average degrees of polymerizations (X_n) and relatively high dispersities ($Đ$). The best (less worse) results appear those of the two most popular DT techniques, ITP (X_n up to ~ 400, but with a relatively high $Đ$ of 1.45 [65]) and RAFT with xanthates (X_n up to ~ 580 for a 56% conversion and a $Đ$ value reported as 1.18 but only at 25% conversion [68]). However, OMRP with $[Co^{II}(acac)_2]$ (already described in some detail in section 3) is an exception. It has yielded polymers with X_n up to ~1630 with $Đ < 1.3$, which is particularly notable because it was achieved under RT conditions with $[R_0(VAc)_nCo^{III}(acac)_2]$ ($n \sim 4$) as monomolecular initiator and the

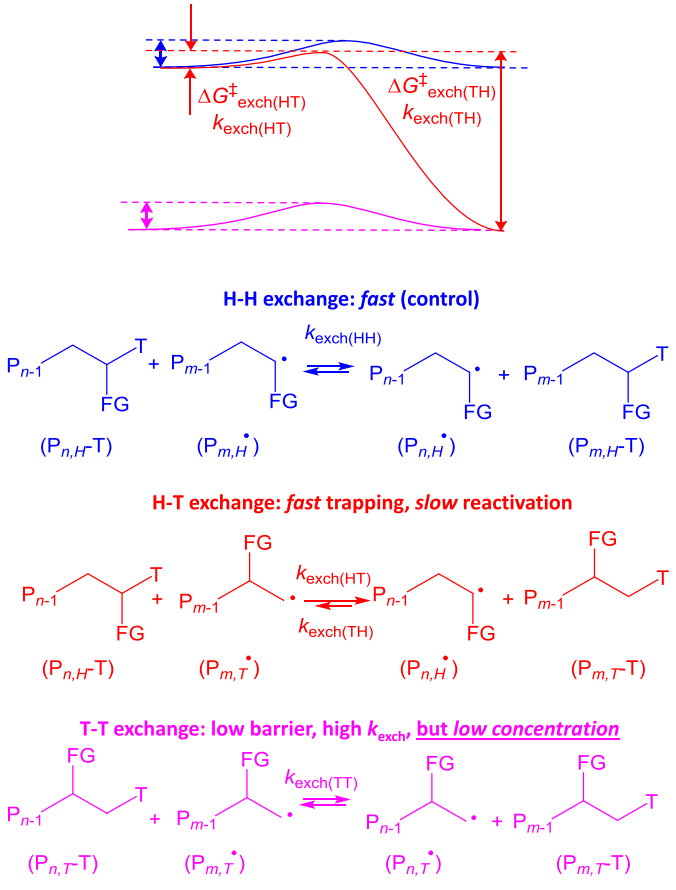

Fig. 7. Mechanisms and energy profiles of the associative exchange processes involving head and tail dormant species with head and tail radicals in controlled polymerization of asymmetric monomers.

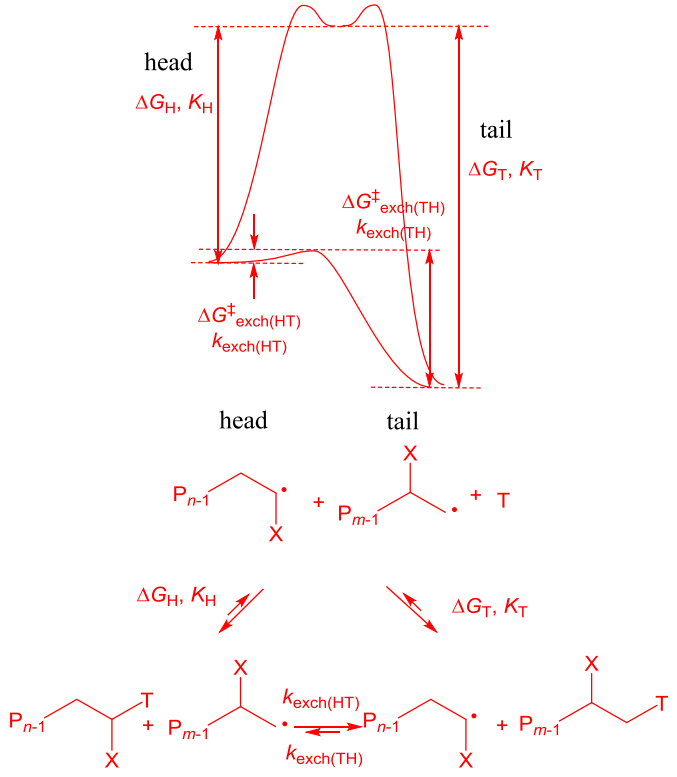

Fig. 8. Thermodynamic cycle involving the non-degenerative head-tail exchange and the dissociative equilibria of the individual head and tail dormant species.

polymerization kinetics did not indicate any significant slowdown [42]. A rationalization of this behavior was possible from a combined experimental and computational study [69]. The possibility that the presence of the cobalt complex somehow leads to a lower impact of the HH and TT defects, which would not be consistent with the polymerization mechanism, was discarded following a careful NMR study of the polymer product. The degree of inverted monomers in the chain backbone revealed by the NMR analysis was indeed as expected (1.2–1.3%). DFT calculations of the Co^{III}–C BDE in model systems of the tail and head dormant species were performed with a variety of different functionals. The results obtained with the BPW91* functional, which is well-suited to systems of variable spin states (the Co^{II} complex with S = 3/2 and the organic radical with S = 1/2 combine to yield the organocobalt(III) product with S = 0), are shown in Fig. 9. As expected, the more reactive tail radical establishes a stronger bond with [Co(acac)$_2$], namely ca. 5 kcal/mol stronger than the head radical. However, the dormant species generation is completed by chelation via the carbonyl group of the metal-bonded monomer, because d^6 Co^{III} has a preference for a saturated octahedral environment. Chelation by the head chain model yields a 5-member chelate ring and provides an estimated stabilization of 6.2 kcal/mol to the system. Chelation by the tail chain model, on the other hand, generates a less stable 6-member chelate ring with an estimated stabilization of only 2.3 kcal/mol. Therefore, the stronger σ bond of the tail radical is associated to a weaker chelation and *vice versa*, the two effects compensating to end up with very similar overall stabilization energies. The use of other functionals provided quite different absolute values for the head and tail BDEs, but in all cases the same compensating effect of homolytic BDE and chelation was observed, yielding a difference between the stabilizing effects close to zero for the two isomers. For other $CH_3CH(OAc)$-T and T-$CH_2CH_2(OAc)$ bonds, on the other hand, no additional phenomenon compensates for the BDE difference, which is much greater and in favor of the tail dormant species (again, different absolute BDE values but quite similar differences were obtained with use of different functionals). Quite obviously, the same chelation effect would operate for this controlling system in the DT regime, because of the arguments presented in section 6, Fig. 8.

8. Effect of bond polarity in the OMRP of VDF

VDF is another asymmetric LAM that leads to inverted monomer addition [57], to an even greater extent than VAc, making it impossible to obtain polymers with high X_n values and low $Đ$ by standard DT techniques such as ITP and RAFT [64,66], while RT methods have not been applied. A significant improvement in the controlled polymerization of this monomer has been provided quite recently by OMRP-RT using, once again, [Co^{II}(acac)$_2$] as moderating agent [70]. In this case, in contrast to the VAc story told in the previous section, predictions by DFT calculations have preceded the experimental work. Chain chelation cannot help for this monomer because the fluorine atoms bonded to carbon in the PVDF chain are not sufficiently strong electron donors to provide any stabilization. The key effect is the influence of the fluorine substitution at C^{α} and C^{β} on the Co–C bond polarity, which is reflected in the cost of the homolytic bond cleavage. The calculated BDEs for the entire series of X-$CF_nH_{2-n}CF_mH_{3-m}$ (n = 0, 1, 2; m = 0, 1, 2, 3)

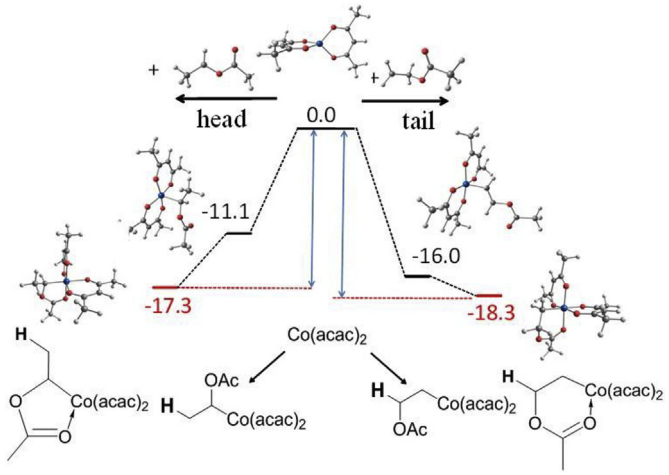

Fig. 9. Energy profile (relative *H* values in kcal/mol) and views of the optimized geometries for the trapping of head and tail PVAc model radicals $CH_3CH(OAc)^{\bullet}$ and $^{\bullet}CH_2CH_2(OAc)$ [69].

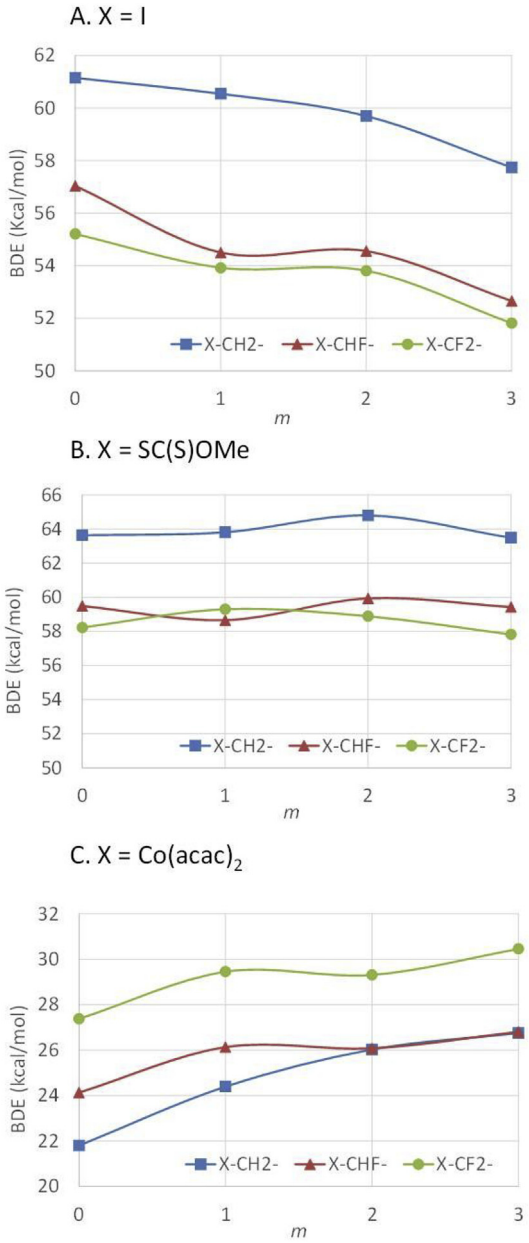

Fig. 10. C-X bond dissociation enthalpies (in kcal/mol) calculated for X-$CF_nH_{2-n}CF_mH_{3-m}$ (A, X = I; B, X = SC(S)OEt; C, X = Co(acac)$_2$; n = 0 (squares), 1 (triangles), 2 (circles); m = 0, 1, 2, 3) by DFT.

molecules, for X = I, SC(S)OMe and $Co(acac)_2$, are shown in Fig. 10 [71]. The iodide series is of relevance for the ITP results and the xanthate series is useful to rationalize the RAFT polymerization results. The DFT chosen method was benchmarked on a number of molecules with X = H, for which experimental BDE values are available [72,73], yielding correct trends and acceptable quantitative agreement. While all observed trends shown in Fig. 10 cannot be fully explained, it is at least possible to advance a likely rationalization for the fact that the X–CH_2R bond is stronger than the X–CF_2R bond for X = I and SC(S)OEt (*i.e.* the X-CH_2- line is above the X-CF_2- line in Fig. 10A and B), whereas the opposite is true for X = $Co(acac)_2$ (Fig. 10C).

The energy required to homolytically break a bond can be decomposed into three contributions (see Scheme 6). This first one is a polar contribution related to the charge redistribution in the bond being broken, from the equilibrium charges of the two atoms in the molecule (δ/ε), for a charge difference $\Delta q = (\delta-\varepsilon)$, to the equilibrium charges of the same atoms in the separate fragments (δ'/ε'), for a charge difference $\Delta q' = (\delta'-\varepsilon')$. The second one is related to orbital overlap and energy difference between the fragment frontier orbitals in the bond cleavage process to produce fragments with the same geometry as in the initial molecule, and the final one is related to the geometry relaxation to yield the two fragments in their most stable geometries. It is not easy to predict the effect that F substituents on C^{α} and C^{β} have on the second contribution while the effect of the third contribution was shown by the DFT calculations to be quantitatively small and to contribute little to the trends shown in Fig. 10. However, the effect on the charge redistribution can be easily predicted. When the atom bonded to carbon is more electronegative (*i.e.* for I and S in the xanthate group), the bond formation displaces charge from C to X ($\varepsilon > \varepsilon'$ and $\delta < \delta'$), hence $\Delta q < \Delta q'$. In this case, the introduction of F substituents (especially at the α position, but also at the β position, particularly for X = I) opposes this electron density flow and reduces the charge redistribution. Conversely, the Co atom in $[Co(acac)_2]$ is more electropositive than the C atom and the bond formation displaces charge from X to C ($\varepsilon < \varepsilon'$ and $\delta > \delta'$), hence $\Delta q > \Delta q'$. Here the introduction of F substituents, both on C^{α} and on C^{β}, helps this electron density flow and thus increases the charge redistribution.

The most interesting comparisons are the predicted BDE values for the X–CF_2CH_3 and X–CH_2CF_2H, models of the head and tail dormant species in VDF polymerizations with the moderating species X, namely $PVDF_H$-X and $PVDF_T$-X. The BDE difference, $\Delta BDE(T\text{-}H) = [BDE(X{-}CH_2CF_2H) - BDE(X{-}CF_2CH_3)]$, is 4.5 kcal/mol for X = I, 6.6 kcal/mol for X = SC(S)OEt, and −1.4 kcal/mol for X = $Co(acac)_2$. These values rationalize rather well the effect of the inverted monomer additions in the VDF ITP and RAFT polymerizations by xanthates, as highlighted above in section 6, and predict that OMRP with $[Co^{II}(acac)_2]$ as moderating agent should lead to better results. This prediction was indeed confirmed by the OMRP-RT implemented with $[R_0(VAc)_nCo^{III}(acac)_2]$ ($n \sim 4$) as monomolecular initiator [70], yielding a PVDF with X_n up to 160 and $Đ < 1.3$, which then led to successful chain extension to yield well-defined PVDF-*b*-PVAc (AB-type diblock) and PVDF-*b*-PVAc-*b*-PVDF (symmetric ABA-type triblock) copolymers. The results shown in Fig. 10 also suggest that the OMRP of other fluorinated monomers, notably trifluoroethylene, mediated by $[Co^{II}(acac)_2]$ should also be successful, which still awaits experimental confirmation.

The DFT calculations on the corresponding X-$CF_nH_{2-n}CF_mH_{3-m}$ series of compounds with X = $Mn(CO)_5$ yields a trend similar to that of $Co(acac)_2$, although with much higher BDE values (ca. 20 kcal/mol greater) [71]. The calculations were also extended to $[Mn(CF_3)(CO)_5]$ and $[Mn(CHF_2)(CO)_5]$, because experimental BDE values for these compounds were available [48,74], but the calculated values were found unacceptably higher. Since the available experimental values had been determined by indirect or approximate methods (Calvet calorimetry, photoionization mass spectrometry), new measurements have been carried out on these compounds, as well as on the newly synthesized $[Mn(CH_2CF_3)(CO)_5]$, by the kinetics study of the homolytic bond cleavage process. These new experimental values are in agreement with the DFT-calculated BDEs [75]. Preliminary VDF polymerization studies in the presence of $[Mn(CF_3)(CO)_5]$ confirm that this compound is able to produce $CF_3^{\bullet}$ radicals under thermal or photochemical (UV or visible light) conditions, producing PVDF in high yields. However, the unstable nature of the $[^{\bullet}Mn(CO)_5]$ moderating species did not provide a sufficient control for this OMRP process.

9. Catalytic chain transfer for LAMs

As shown in section 2, CCT potentially interferes with controlled chain growth in OMRP, in some cases even becoming the predominant phenomenon. CCT leads to short-chain polymers with unsaturated chain ends, which are valuable commodities. They have a number of interesting applications related to the controlled reduction of the molecular weight and to the possible use as macromonomers for graft polymers or for alternative chain-end functionalization [27]. Obtaining such materials for LAMs is less facile than for more activated monomers. CCT is particularly effective for methacrylates, methacrylonitrile, α-methylstyrene and other monomers yielding tertiary radicals, namely radicals that do not form strong bond with metals in the OMRP dormant species [27,28] and becomes increasingly difficult as the formation of the OMRP dormant species becomes more favorable, because the concentration of the active metal catalyst decreases. Thus, the key to promote CCT for LAMs is to employ metal complexes with which even the strong radicals associated to these monomers cannot establish strong bonds. We have recently shown the first evidence (in the open literature) for catalytic chain transfer in the polymerization of VAc [76], preceded only by a claim in an early patent [77]. This observation has followed our exploration of ligand effects for

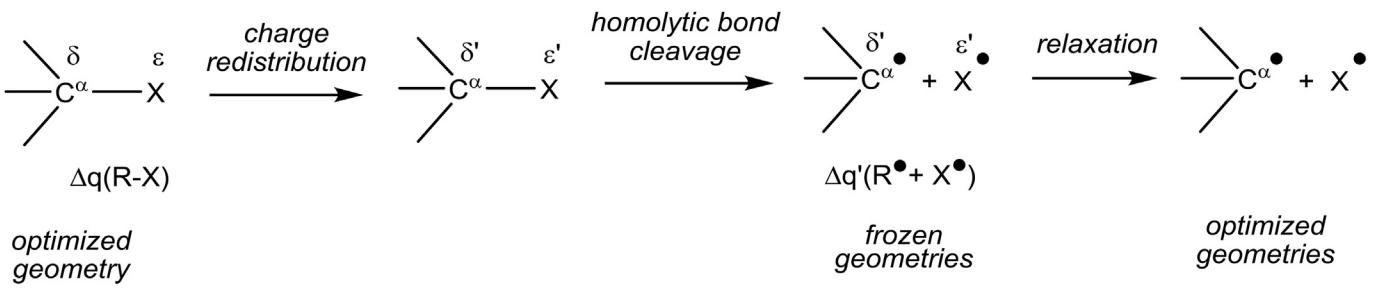

Scheme 6. Ideal three-step process for the homolytic cleavage of a C-X bond.

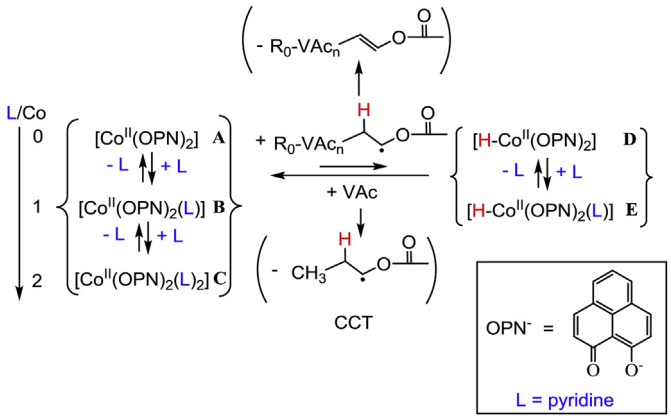

Scheme 7. Mechanism of [Co^{II}(OPN)$_2$]-catalyzed chain transfer (CCT) in VAc polymerization and effect of L coordination.

the cobalt(II) bis(β-diketonate) moderating system. Using the 9-hydroxyphenalenone as ligand precursor, the resulting [Co^{II}(OPN)$_2$] complex (OPN = 9-oxyphenalenone) gave evidence of weaker interaction with the growing PVAc$^•$ chains relative to [Co^{II}(acac)$_2$] and even to [Co^{II}(tmhd)$_2$] (see section 4, Fig. 5), since the polymerization carried out with the dual V-70/[Co^{II}(OPN)$_2$] initiating system did not reveal any induction time under anhydrous conditions. The produced macromolecules have lower molecular weights than predicted by the monomer/Co ratio, which did not increase with monomer conversion, and their MALDI-TOF analysis revealed both R_0 (from V-70) and H (from CCT) α-chain ends. The lowest molecular weights (highest catalytic efficiency) were found in the presence of moderate amounts of added pyridine (L). These results are rationalized as shown in Scheme 7. Both the 4-coordinate [Co^{II}(OPN)$_2$], **A**, and the 5-coordinate monoligand adduct [Co^{II}(OPN)$_2$(L)], **B**, can abstract a β-H atom from the growing PVAc$^•$ radical chain to yield the hydride species [Co^{III}H(OPN)$_2$], **D**, and [Co^{III}H(OPN)$_2$(L)], **E**, respectively, but the 6-coordinate bis(ligand) adduct [Co^{II}(OPN)$_2$(L)$_2$], **C**, does not possess the needed vacant site and is therefore inactive. The increased CCT activity upon addition of small pyridine amounts is consistent with **B** being more active than **A**, whereas a large pyridine excess shifts the Co^{II} equilibria toward species **C** and the activity decreases. These recent results bode well for the further development of efficient CCT processes for LAMs.

10. Conclusions

Organometallic species featuring homolytically weak metal-carbon bonds are of great utility as labile dormant species in controlled radical polymerization (OMRP), particularly for "less-activated monomers" (LAMs). In this area of organometallic chemistry, the metal-carbon bond weakness is an advantage rather than a nuisance. It is easier for metal complexes in OMRP, relative to other moderating agents used in more popular RDRP techniques, to engineer systems able to promote, in the dormant species, homolytic bond cleavage to liberate the free carbon-based radical (in "reversible termination" or RT methods), or the associative radical exchange (in "degenerative transfer" or DT methods). Metal complexes have provided additional handles, not available for other moderating systems, to cope with the problem of monomer addition "errors", *i.e.* inverted monomer additions, for asymmetric LAMs leading to isomeric "head" and "tail" dormant species. These handles are based on coordination chemistry principle (availability of coordination sites, chelation equilibria) and on the bond polarity switching by the less electronegative metal atom. They are *ad hoc* solutions, valid only for certain monomers. However, the intelligent use and extension of these handles to yet unexplored monomers is an available resource to be kept in mind. The nuisance of having to use the stoichiometric amount (chainwise) of metal and having to post-modify the isolated polymer to remove the metal from the ω-chain end may be tolerated, if the polymer material has sufficiently high added value and if it is accessible with the desired chain length, molecular weight distribution and chain-end fidelity only by the OMRP method. Finally, when the strength of the metal-carbon bond is decreased to the point that radical chain trapping becomes insufficient to control the macromolecular chain growth, the profitable process of catalytic chain transfer (CCT) to monomer may become accessible, even for the more reactive radicals associated to LAMs. In this case, the metal complex has a catalytic role like in ATRP and is not consumed stoichiometrically. This is an area that presents opportunities for interesting further developments.

Acknowledgements

The research topic highlighted in this article has been developed in the main author's laboratory over the past 20 years in large part in collaboration with polymer scientists, too many to be listed (but several ones may be found in the references). All of them are warmly thanked for their teaching, inspiration, student exchange and a lot of excitement in our joint endeavors. Our research efforts have been generously supported by various grants from the ANR (Agence Nationale de la Recherche), by recurring funds, a PICS (Projet International de Coopération Scientifique) and an LIA (Laboratoire International Associé) from CNRS (Centre National de la Recherche Scientifique), and by access to the computing resources of CINES and IDRIS by GENCI (Grand Équipement National de Calcul Intensif) and to the resources of CALMIP by the CICT (Centre Interuniversitaire de Calcul de Toulouse).

Appendix A. Supplementary data

Supplementary data to this article can be found online at https://doi.org/10.1016/j.jorganchem.2018.11.012.

References

[1] K. Bernhauer, O. Mueller, F. Wagner, Angew. Chem. Int. Ed. 75 (1963) 1145–1156.
[2] S. Bhaduri, D. Mukesh, Homogeneous Catalysis: Mechanisms and Industrial Applications, second ed., John Wiley & Sons, Hoboken, New Jersey, 2014.
[3] J.P. Collman, L.S. Hegedus, J.R. Norton, R.G. Finke, Principles and Applications of Organotransition Metal Chemistry, second ed., University Science Books, Mill Valley, California, 1987.
[4] R.H. Crabtree, The Organometallic Chemistry of the Transition Metals, sixth ed., Wiley, Hoboken, New Jersey, 2014.
[5] A.D. Jenkins, R.G. Jones, G. Moad, Pure Appl. Chem. 82 (2010) 483–491.
[6] K. Matyjaszewski, Y. Gnanou, L. Leibler, Macromolecular Engineering: Precise Synthesis, Materials Properties, Applications, Wiley-VCH Verlag GmbH, 2007.
[7] S. Maria, F. Stoffelbach, J. Mata, J.-C. Daran, P. Richard, R. Poli, J. Am. Chem. Soc. 127 (2005) 5946–5956.
[8] H. Fischer, Chem. Rev. 101 (2001) 3581–3610.
[9] T. Aida, Prog. Polym. Sci. 19 (1994) 469–528.
[10] R. Poli, Angew. Chem. Int. Ed. 45 (2006) 5058–5070.
[11] A. Debuigne, R. Poli, C. Jérôme, R. Jérome, C. Detrembleur, Prog. Polym. Sci. 34 (2009) 211–239.
[12] K.M. Smith, W.S. McNeil, A.S. Abd-El-Aziz, Macromol. Chem. Phys. 211 (2010) 10–16.
[13] M. Hurtgen, C. Detrembleur, C. Jerome, A. Debuigne, Polym. Rev. 51 (2011) 188–213.
[14] R. Poli, Organometallic mediated radical polymerization, in: K. Matyjaszewski, M. Möller (Eds.), Polymer Science: a Comprehensive Reference, Elsevier BV, Amsterdam, 2012, pp. 351–375.
[15] C.-H. Peng, T.-Y. Yang, Y. Zhao, X. Fu, Org. Biomol. Chem. 12 (2014) 8580–8587.
[16] R. Poli, L.E.N. Allan, M.P. Shaver, Prog. Polym. Sci. 39 (2014) 1827–1845.

[17] L.E.N. Allan, M.R. Perry, M.P. Shaver, Prog. Polym. Sci. 37 (2012) 127–156.
[18] R. Poli, Chem. Eur J. 21 (2015) 6988–7001.
[19] R. Poli, Organometallic mediated radical polymerization, in: Reference Module in Materials Science and Materials Engineering, Elsevier, 2016.
[20] A. Debuigne, C. Jerome, C. Detrembleur, Polymer 115 (2017) 285–307.
[21] B.B. Wayland, G. Poszmik, S. Mukerjee, J. Am. Chem. Soc. 116 (1994) 7943–7944.
[22] L.D. Arvanatitopoulos, M.P. Greuel, H.J. Harwood, Polym. Prepr. (Am. Chem. Soc., Div. Polym. Chem.) 35 (1994) 549–550.
[23] L.D. Arvanitopoulos, M.P. Greuel, B.M. King, A.K. Shim, H.J. Harwood, ACS Symp. Ser. 685 (1998) 316–331.
[24] B.B. Wayland, G. Poszmik, M. Fryd, Organometallics 11 (1992) 3534–3542.
[25] B.B. Wayland, S. Mukerjee, G. Poszmik, D.C. Woska, L. Basickes, A.A. Gridnev, M. Fryd, S.D. Ittel, ACS Symp. Ser. 685 (1998) 305–315.
[26] Y.G. Zhao, S.L. Zhang, Z.Q. Wu, X. Liu, X.Y. Zhao, C.H. Peng, X.F. Fu, Macromolecules 48 (2015) 5132–5139.
[27] A.A. Gridnev, S.D. Ittel, Chem. Rev. 101 (2001) 3611–3659.
[28] S. Slavin, K. McEwan, D.M. Haddleton, Cobalt-catalyzed chain transfer polymerization: a review, in: K. Matyjaszewski, M. Möller (Eds.), Polymer Science: a Comprehensive Reference, Elsevier BV, Amsterdam, 2012, pp. 249–274.
[29] J.S. Wang, D. Greszta, K. Matyjaszewski, Abstr. Pap. Am. Chem. Soc. 210 (1995), 227-PMSE.
[30] M. Kato, M. Kamigaito, M. Sawamoto, T. Higashimura, Macromolecules 28 (1995) 1721–1723.
[31] The OMRP acronym, now universally accepted, was actually introduced only in 2006, see Ref. [10].
[32] E. Le Grognec, J. Claverie, R. Poli, J. Am. Chem. Soc. 123 (2001) 9513–9524.
[33] W.A. Braunecker, Y. Itami, K. Matyjaszewski, Macromolecules 38 (2005) 9402–9404.
[34] W.A. Braunecker, W.C. Brown, B. Morelli, W. Tang, R. Poli, K. Matyjaszewski, Macromolecules 40 (2007) 8576–8585.
[35] M.P. Shaver, L.E.N. Allan, H.S. Rzepa, V.C. Gibson, Angew. Chem. Int. Ed. 45 (2006) 1241–1244.
[36] L.E.N. Allan, M.P. Shaver, A.J.P. White, V.C. Gibson, Inorg. Chem. 46 (2007) 8963–8970.
[37] R. Poli, M.P. Shaver, Chem. Eur J. 20 (2014) 17530–17540.
[38] L.E.N. Allan, J.P. MacDonald, A.M. Reckling, C.M. Kozak, M.P. Shaver, Macromol. Rapid Commun. 33 (2012) 414–418.
[39] L.E.N. Allan, J.P. MacDonald, G.S. Nichol, M.P. Shaver, Macromolecules 47 (2014) 1249–1257.
[40] R. Poli, M.P. Shaver, Inorg. Chem. 53 (2014) 7580–7590.
[41] Z. Lu, M. Fryd, B.B. Wayland, Macromolecules 37 (2004) 2686–2687.
[42] A. Debuigne, Y. Champouret, R. Jérôme, R. Poli, C. Detrembleur, Chem. Eur J. 14 (2008) 4046–4059.
[43] S. Yamago, Chem. Rev. 109 (2009) 5051–5068.
[44] A. Debuigne, J.R. Caille, R. Jérôme, Angew. Chem. Int. Ed. 44 (2005) 1101–1104.
[45] S. Maria, H. Kaneyoshi, K. Matyjaszewski, R. Poli, Chem. Eur J. 13 (2007) 2480–2492.
[46] A. Debuigne, R. Poli, R. Jérôme, C. Jérôme, C. Detrembleur, ACS Symp. Ser. 1024 (2009) 131–148.
[47] F.S. Wang, T.Y. Yang, C.C. Hsu, Y.J. Chen, M.H. Li, Y.J. Hsu, M.C. Chuang, C.H. Peng, Macromol. Chem. Phys. 217 (2016) 422–432.
[48] J.A. Martinho Simões, J.L. Beauchamp, Chem. Rev. 90 (1990) 629–688.
[49] J.L. Hodgson, C.Y. Lin, M.L. Coote, S.R.A. Marque, K. Matyjaszewski, Macromolecules 43 (2010) 3728–3743.
[50] Y. Champouret, U. Baisch, R. Poli, L. Tang, J.L. Conway, K.M. Smith, Angew. Chem. Int. Ed. 47 (2008) 6069–6072.
[51] Y. Champouret, K.C. MacLeod, U. Baisch, B.O. Patrick, K.M. Smith, R. Poli, Organometallics 29 (2010) 167–176.
[52] K.S. Santhosh Kumar, Y. Gnanou, Y. Champouret, J.-C. Daran, R. Poli, Chem. Eur J. 15 (2009) 4874–4885.
[53] C.H. Peng, J. Scricco, S. Li, M. Fryd, B.B. Wayland, Macromolecules 41 (2008) 2368–2373.
[54] C.S. Hsu, T.Y. Yang, C.H. Peng, Polym. Chem. 5 (2014) 3867–3875.
[55] M. Hurtgen, A. Debuigne, C. Jerome, C. Detrembleur, Macromolecules 43 (2010) 886–894.
[56] P.J. Flory, F.S. Leutner, J. Polym. Sci. 3 (1948) 880–890.
[57] J. Guiot, B. Ameduri, B. Boutevin, Macromolecules 35 (2002) 8694–8707.
[58] J. Xia, H.-j. Paik, K. Matyjaszewski, Macromolecules 32 (1999) 8310–8314.
[59] M. Wakioka, K.Y. Baek, T. Ando, M. Kamigaito, M. Sawamoto, Macromolecules 35 (2002) 330–333.
[60] Y. Kwak, A. Goto, T. Fukuda, Y. Kobayashi, S. Yamago, Macromolecules 39 (2006) 4671–4679.
[61] C. Dommanget, F. D'Agosto, V. Monteil, Angew. Chem. Int. Ed. 53 (2014) 6683–6686.
[62] A. Kermagoret, A. Debuigne, C. Jerome, C. Detrembleur, Nat. Chem. 6 (2014) 179–187.
[63] M. Destarac, D. Charmot, X. Franck, S.Z. Zard, Macromol. Rapid Commun. 21 (2000) 1035–1039.
[64] M. Guerre, B. Campagne, O. Gimello, K. Parra, B. Améduri, V. Ladmiral, Macromolecules 48 (2015) 7810–7822.
[65] M.C. Iovu, K. Matyjaszewski, Macromolecules 36 (2003) 9346–9354.
[66] C. Boyer, D. Valade, L. Sauguet, B. Améduri, B. Boutevin, Macromolecules 38 (2005) 10353–10362.
[67] M. Guerre, S.M.W. Rahaman, B. Améduri, R. Poli, V. Ladmiral, Macromolecules 49 (2016) 5386–5396.
[68] M.H. Stenzel, L. Cummins, G.E. Roberts, T.P. Davis, P. Vana, C. Barner-Kowollik, Macromol. Chem. Phys. 204 (2003) 1160–1168.
[69] A.N. Morin, C. Detrembleur, C. Jérôme, P.D. Tullio, R. Poli, A. Debuigne, Macromolecules 46 (2013) 4303–4312.
[70] S. Banerjee, V. Ladmiral, A. Debuigne, C. Detrembleur, R. Poli, B. Améduri, Angew. Chem. Int. Ed. 57 (2018) 2934–2937.
[71] R. Poli, S.M.W. Rahaman, V. Ladmiral, B. Améduri, J. Organomet. Chem. 864 (2018) 12–18.
[72] W.R. Dolbier, Chem. Rev. 96 (1996) 1557–1584.
[73] D.F. McMillen, D.M. Golden, Annu. Rev. Phys. Chem. 33 (1982) 493–532.
[74] J.A. Connor, M.T. Zafaranimoattar, J. Bickerton, N.I. Elsaied, S. Suradi, R. Carson, G. Altakhin, H.A. Skinner, Organometallics 1 (1982) 1166–1174.
[75] R. Morales-Cerrada, C. Fliedel, J.-C. Daran, F. Gayet, V. Ladmiral, B. Améduri, R. Poli, Chem. Eur J. (2018). https://doi.org/10.1002/chem.201804007.
[76] E.V. Bellan, L. Thevenin, F. Gayet, C. Fliedel, R. Poli, ACS Macro Lett. 6 (2017) 959–962.
[77] A.H. Janowicz, U.S. Patent 4694054, (1991).